



INTERNATIONAL JOURNAL OF ENGINEERING SCIENCES & RESEARCH TECHNOLOGY

INTENSIFICATION OF HEAT TRANSFER AND FLOW IN HEAT EXCHANGER WITH SHELL AND HELICALLY COILED TUBE BY USING NANO FLUIDS

Dr. Khalid Faisal Sultan*, Karema Assi Hamad

* Electromechanical. Eng. Dept University of Technology
Electromechanical. Eng. Dept University of Technology

ABSTRACT

This article presents an experimental study on enhancement of heat transfer and pressure drop of nanofluids flow. In this study the method using to enhancement of heat transfer and pressure drop, by used the helically coiled tube heat exchange and the nanofluids instead of the base fluid (oil). The concentrations of nanofluid used are ranging from (5 – 30 wt%). The shell of the heat exchanger is constant wall temperature (CWT) . Two types of nanoparticles used in this paper silver (Ag (30nm)) and Titanium Oxide (TiO₂ (50nm)) as well as the base fluid (oil). The effect of different parameters such as flow Reynolds number, nanofluid temperature, concentration and type of nanoparticle on heat transfer coefficient and pressure drop of the flow are studied at constant wall temperature. The obtained results show an increase in heat transfer coefficient of 45.35% for Ag + oil and 32.29% for TiO₂ + oil at concentration of 30 wt % compared with base fluid (oil). The heat transfer coefficient and pressure drop is increased by using nanofluids (Ag, TiO₂ – oil) instead of the base fluid (oil). In addition the results indicated that by using heat exchanger with shell and helically coiled tube, the heat transfer performance is improved as well as the pressure drop enhancement due to the curvature of the tube. Furthermore, a maximum increase of 34.15% (Ag + Oil) and 27.23% (TiO₂+ Oil) in Nusselt number ratio for a range of Reynolds numbers between 20 and 200. This paper decided that the nanofluid behaviors are close to typical Newtonian fluids through the relationship between viscosity and shear rate. Moreover to performance index are used to present the corresponding flow and heat transfer technique. The type and size nanoparticles play an important role in enhancement of heat transfer rate.

KEYWORDS: Nanofluids, Spiral tube heat exchange, Convective heat transfer, Pressure drop.

INTRODUCTION

Thermal load removal is a great concern in many industries including power plants, production and chemical processes, transportation and electronics. In order to meet the ever increasing need for cooling the high heat flux surfaces, different enhanced heat transfer techniques have been suggested. Most of these methods are based on structure variation, vibration of heated surface, injection or suction of fluid and applying electrical or magnetic fields which are well documented in literature [1,2]. However, applying these enhanced heat transfer techniques is no longer feasible for cooling requirement of future generation of microelectronic systems, since they would result in undesirable cooling system size and low efficiency of heat exchangers. To obviate this problem, nanofluids with enhanced thermo-fluidic properties have been proposed since the past decade. Nanofluid is a uniform dispersion of nanometer sized particles inside a liquid which was first pioneered by Choi [3]. Excellent characteristics of nanofluids such as enhanced thermal conductivity, long time stability and little penalty in

pressure drop increasing and tube wall abrasion have motivated many researchers to study on thermal and flow behavior of nanofluids. These studies are mainly focused on effective thermal conductivity, phase change behavior, tribological properties, flow and convective heat transfer of nanofluids. A wide range of experimental and theoretical studies has been performed on effective thermal conductivity of nanofluids within past decade. In these studies, the effect of different parameters such as particle concentration, particle size, mixture temperature and Brownian motion on thermal conductivity of nanofluids was investigated. The results showed an increase in thermal conductivity of nanofluid with the increase of nanoparticles concentration and mixture temperature [4–7]. Also it was shown that larger enhancement in thermal conductivity is attributed to the finer particle size [6–8]. Due to the enhanced thermal properties of nanofluids, majority of recent studies are focused on convective heat transfer behavior of nanofluids in laminar and turbulent flows. Almost all of these works report the enhancement of

nanofluid convective heat transfer. Several numerical and experimental studies have considered nanofluid convective heat transfer in turbulent flow [9–12]. Some other studies have investigated the convective heat transfer of nanofluids in laminar flow. Wen and Ding [13] have studied Al₂O₃/water nanofluid heat transfer in laminar flow under constant wall heat flux and reported an increase in nanofluid heat transfer coefficient with the increase in Reynolds number and nanoparticles concentration particularly at the entrance region. Convective heat transfer of CNT nanofluids in laminar regime with a constant heat flux wall boundary condition was investigated by Ding et al. [14]. They observed a maximum enhancement of 350% in convective heat transfer coefficient of 0.5 wt.% CNT/water nanofluid at Re=800. In addition, a few works have studied friction factor characteristics of nanofluids flow besides the convective heat transfer. Xuan and Li [15] investigated the flow and convective heat transfer characteristics for Cu/water nanofluids inside a straight tube with a constant heat flux at the wall, experimentally. Results showed that nanofluids give substantial enhancement of heat transfer rate compared to pure water. They also claimed that the friction factor for the nanofluids at low volume fraction did not produce extra penalty in pumping power. In laminar flow, Chandrasekar et al. [16] investigated the fully developed flow convective heat transfer and friction factor characteristics of Al₂O₃/water nanofluid flowing through a uniformly heated horizontal tube with and without wire coil inserts. They concluded that for the nanofluid with a volume concentration of 0.1%, the Nusselt number increased up to 12.24% compared to that of distilled water. However, the friction factors of the same nanofluid were almost equal to those of water under the same Reynolds numbers. Another technique which is employed for heat transfer augmentation is using helical tubes instead of straight tubes. Due to their compact structure and high heat transfer coefficient, helical tubes have been introduced as one of the passive heat transfer enhancement techniques and are widely used in various industrial applications such as heat recovery processes, air conditioning and refrigeration systems, chemical reactors, food and dairy processes. Single-phase heat transfer characteristics in the helical tubes have been widely studied by researchers both experimentally and

theoretically. The heat transfer rates between a helically coiled heat exchanger and a straight tube heat exchanger were compared by Prabhajan et al. [17]. Results showed that the geometry of the heat exchanger and the temperature of the water bath surrounding the heat exchanger affected the heat transfer coefficient. Xin et al. [18] studied the effects of coil geometries and the flow rates of air and water on pressure drop in both annular vertical and horizontal helical pipes. The test sections with three different diameters of inner and outer tubes were tested. The results showed that the transition from laminar to turbulent flow covers a wide Reynolds number range. On the basis of the experimental data, a correlation of the friction factor was developed. The maximum deviation of the friction factor from experiments and the correlation was found to be 15%. Choi and colleagues [19] used spherical and rod shape Al₂O₃ and spherical AlN nanoparticles dispersed in transformer oil to make nanofluids. All three types of nanofluids showed a small enhancement in the heat transfer coefficient at a Reynolds number range of 100 to 500. A maximum of 20% increase was observed for the AlN/transformer oil based nanoparticles at a volume fraction of 0.5%.

The objects of this article, examine the various factors that could potentially impact the enhancement of heat transfer coefficients of oil – based nanofluid including nanoparticle size, volume fraction, Reynolds number and nanofluid temperature.

NANOFLUID PREPARATION

The studied nanofluid is formed by silver (Ag (30 nm)) and titanium oxide (TiO₂) (50nm) nanoparticles and the two – step method was used to prepare nanofluids. Nanofluid samples were prepared by dispersing pre – weighed quantities of dry Particles in base fluid (oil). In a typical procedure, the pH of each nanofluids a mixture was measured (pH = 4.3 – 4.5).The mixtures were then subjected to ultrasonic mixing [100 kHz, 300 W at 25 – 30 C0, Toshiba, England] for one hour to break up any particle aggregates. The nanofluid of this study was included 20W50 engine oil (Castrol Company) (GTX) and nanoparticles (US Research Nano materials, Inc). Their properties are shown in table 1 ,2 and 3 respectively

Table1: The properties of engine oil [20]

Name	SAE 20W50
Density at 15.6°C (kg/m ³)	893
Viscosity at 100°C (cSt)	17
Viscosity index	115
Total alkalinity (mgKOH/g)	6
Minimum ignition point	214
Minimum Pour point (°C)	- 24

Table2: The properties of Nano powder Cu [21]

Silver Nano powder Ag, 99%, 30 nm	
Purity	>99%
crystal phases	Monoclinic
APS	30 nm
SSA	20– 40 m ² /g
Color	Lead
Morphology	Nearly spherical
True density	10.500 g/cm ³

Table3: The properties of Nano powder TiO2 [21]

Titanium oxide Nano powder TiO ₂ , 99%, 50 nm	
Purity	>99%
crystal phases	Monoclinic
APS	50nm
SSA	20 – 40 m ² /g
Color	white
Morphology	spherical
True density	4.250 g /cm ³

An image nanofluids containing silver (Ag (30 nm)) and titanium oxide (TiO₂) (50 nm) is display in Fig .1. Nanofluids with different weight percent ($\Phi = 5, 10, 20,$ and 30 wt %).



Fig.1 Show nanofluids for Ag + Oil , TiO₂ + Oil and Oil

EXPERIMENTAL SETUP

The experimental set up consist of the heat exchanger is made of Pyrex (soft glass) and test section has the helically tube 10 mm inner, 12 mm outer diameters , 34 turns and length of coil is 750 mm shell has 70 mm inner, 80 mm outer diameters and 1000 mm length. The set – up has helically coiled tube side loop and shell side loop. The helically coiled tube side loop handles two types of nanofluids used silver – oil, and titanium oxide. Shell side loop handles hot water. Shell side loop consist of storage vessel of 20 L capacity with heater of 4.5 Kw, control valve ,pump and thermostat. The helically coiled tube side loop consists of test section containing shell and spiral tube, pump [Bosch 1046 – AE], needle valve , flow meter (Dwyer series MMA mini – master flow meter) having a range of (0.01 – 3.5 LPM), cooling unit and storage vessel of 10 L capacity. The temperature of hot water in the shell side storage vessel is maintained by thermostat. Four T – type thermocouples of 0.15 0C accuracy are used to measure inlet and outlet temperatures of shell and tube side. The shell of the heat exchanger is constant wall temperature (CWT) . The thermocouples are placed and glued with epoxy to avoid leakage. The pressure gauges are placed across the helical tube to measure the pressure drop. The shell is insulated with Acrylic resin coated fiberglass sleeving to minimize the heat loss from shell to the ambient. Distilled water was tested prior to nanofluid

after completion of construction and calibration of the flow loop, testing of the loop's functionality for measuring Nusselt number and viscous pressure loss. The number of the total tests were 200. Hot water and cold water were passed to shell side and tube side to check the leakages in the circuit and tested the thermocouples and thermostat. Hot water was circulated to the shell side. The nanofluids (Ag + Oil and TiO₂ + Oil) at ($\Phi=5, 10, 20,$ and 30 wt %). weight concentration was circulated through the spiral tube side. Shell side pump is switched on when water reaching to a prescribed temperature. This done by thermostat attached in distilled water storage system. The flow configuration was made parallel flow condition. The corresponding temperatures were recorded after attaining the steady state. The same procedure was done for nanofluid at 5 wt % weight concentration. The flow configuration is changed from parallel to counter flow. The same procedure is followed and the temperatures are recorded. Flow rate on shell side (2.25 LPM) and coiled tube pitch are maintained constant throughout the test. The flow rate on tube side is varied. The flow in coil tube side is in the range of 0.75 – 2 LPM. A photograph of the experimental rig is show in the figure.(2), for convective heat transfer and flow characteristics of the nanofluid. As well as the test section for experiment set up as shown in figure. (3).



Fig .2.The experimental system of the convective heat transfer and flow characteristics for nanofluids



Fig (3).The test section for second experiment set up

MEASUREMENT OF THERMAL PROPERTIES NANOFLUID

All physical properties of the nanofluids (Ag, TiO₂ + oil) and oil needed to calculate the pressure drop and the convective heat transfer are measured. The dynamic viscosity (μ) is measured using brook field digital viscometer model DV – E. The thermal conductivity, specific heat and density are measured by Hot Disk Thermal Constants Analyzer(6.1), specific heat apparatus (ESD – 201) as well as the measurement of density was carried out by weighing a sample and volume. The thermal properties of

nanofluids dynamic viscosity (μ), thermal conductivity, specific heat and density are measured with different weight concentrations at ($\Phi= 5, 10, 20,$ and 30 wt %). The empirical relation used in this study to comparison with the practical measurements for nanofluid properties. The thermo physical properties of nanofluid were calculated at the average bulk temperature of the nanofluid by the following equations. The figures (4 – 7) reveal density, viscosity, specific heat, and thermal conductivity for the two types of nanofluid (Ag + oil) and (TiO₂ +oil). The volume fraction (Φ) of the nanoparticles is defined by.

$$\phi = \frac{v_p}{v_p + v_f} = m \frac{\pi d^3}{6 p} \quad (1)$$

Density [22].

$$\rho_{nf} = \Phi \rho_s + (1 - \Phi) \rho_{oil} \quad (2)$$

Viscosity [22].

$$\mu_{nf} = (1 + 2.5\Phi) \mu_{oil} \quad (3)$$

Specific heat [22].

$$Cp_{nf} \rho_{nf} = \Phi(\rho_s Cp_s) + (1 - \Phi)(\rho_{oil} Cp_{oil}) \quad (4)$$

Recently Chandrasekar et al.[23] presented an effective thermal conductivity model (Eq.5)

$$\frac{k_{nf}}{k_{oil}} = \left[\frac{Cp_{nf}}{Cp_{oil}} \right]^{-0.023} \left[\frac{\rho_{nf}}{\rho_{oil}} \right]^{1.358} \left[\frac{\mu_{oil}}{\mu_{nf}} \right]^{0.126} \quad (5)$$

DATA PROCESSING AND VALIDATION

The heat transfer for water and nanofluid are estimated from Eqs.(6) and (7). The average heat transfer is taken for this analysis. Fouling factor was not taken into account.

$$Q_w = m_w Cp_w (T_{in} - T_{out})_w \quad (6)$$

$$Q_{nf} = m_{nf} Cp_{nf} h_{nf} (T_{in} - T_{out})_{nf} \quad (7)$$

$$q = \frac{Q_w + Q_{nf}}{2} \quad (8)$$

The overall heat transfer coefficient, U_o , was calculated from the temperature data and the heat transfer rate using the following equation [24]:

$$U_o = \frac{q}{A_o \text{LMTD}} \quad (9)$$

Where: A_o is the surface area; q is the heat transfer rate; and LMTD is the log mean temperature difference based on the inlet temperature difference, ΔT_1 , and the outlet temperature difference, ΔT_2 .

$$\text{LMTD} = \frac{(\Delta T_2 - \Delta T_1)}{\ln\left(\frac{\Delta T_2}{\Delta T_1}\right)} \quad (10)$$

$$Q = h_i A_i (T_w - T_b) \quad (11)$$

$$\text{Nu}_i = \frac{h_i d_i}{k_{nf}} \quad (12)$$

The overall heat transfer coefficient and inner heat transfer coefficient of coiled tube are calculated from Eqs.(9) and (11). The experimental tube side Nusselt number is calculated from Eq.(12). It measures the convective heat transfer in the helical tube. The overall heat transfer coefficient can be related to the inner and outer heat transfer coefficients by the following equation [24]:

$$\frac{1}{U_o} = \frac{A_o}{A_i h_i} + \frac{A_o \ln\left(\frac{D_i}{d}\right)}{2\pi KL} + \frac{1}{h_o} \quad (13)$$

Where: D_i is the inner diameter of the shell; d is the diameter of the inner spiral tube; K is the thermal

RESULTS AND DISCUSSION

In order to verify the accuracy and the reliability of the experimental system, the heat transfer coefficients are experimentally measured using base oil as the working fluid before obtaining those of oil based Ag and TiO₂ nanofluids. The results of the experimental heat transfer coefficient and pressure drop are compared

conductivity of the Pyrex wall; and L is the length of the heat exchanger.

The Nusslet number in shell side is determined by the following definition .

$$\text{Nu}_o = \frac{h_o D_h}{k_{nf}} \quad (14)$$

Where: D_h is the hydraulic diameter of shell which is calculated from the following formula:

$$D_h = \frac{4(V_{\text{shell}} - V_{\text{tube}})}{\pi(D + d)(L_{\text{shell}} + L_{\text{tube}})} \quad (15)$$

Similarly to the heat transfer coefficient, The friction factor for laminar flow inside helical coiled tube can for range of Dean number (De) of ($11.6 < De < 2000$) is correlated as: [25].

$$\frac{f}{f_s} = \left[1 - \left[1 - \left(\frac{11.6}{De} \right)^{0.45} \right]^{2.22} \right]^{-1} \quad (16)$$

Where:

$$De = \text{Re} \sqrt{\left(\frac{d}{De} \right)}$$

f_s : is friction factor for straight tube it is calculated for

$$\text{laminar flow as } f_s = \frac{64}{\text{Re}}$$

The friction factor for turbulent flow in helical coiled tube, f , is determined as [25].

$$f_e = \frac{7.0144}{\text{Re}} \sqrt{De} \quad (17)$$

The pressure drop of nanofluid flowing inside the coil tubes is evaluated as

$$\Delta p = f \frac{L \rho V^2}{D \cdot 2} \quad (18)$$

with those obtained from the the Shokouhmand , Salimpour [26] ,Salimpour [27], Seban and Metauchlin [25]. for flow in helical coiled heat exchanger which are defined as follows.

$$\text{Nu}_i = 0.112 \text{De}^{0.51} \gamma^{-0.37} \text{Pr}^{0.72} \quad (19)$$

$$Nu_o = 5.48 Re_o^{0.511} \gamma^{0.546} Pr^{0.226} \quad (20)$$

Fig.8 shows the variation of theoretical values with experimental values for heat transfer coefficient. As well as it is seen from this figure, good agreement between these values. Fig. 9 shows the variation of the theoretical values for pressure drop along the test section versus measured pressure drop. The experiments are done at the same condition explained in the heat transfer validation. As it can be seen from Fig. 9, the deviation of the experimental data from the theoretical one is within -2% and +3%. Having established confidence in the experimental system, the heat transfer and pressure drop characteristics of oil – based Ag, TiO₂ nanofluids flowing inside the helical tube is investigate experimentally for laminar flow conditions under constant wall temperature. Note that in the following results, heat transfer and pressure drop data for each two specific cases are not achieved under exactly the same Reynolds numbers. This is because the viscosity of oil based nanofluid is so dependent on fluid temperature and particle volume fraction.

The counter flow versus the parallel flow overall heat transfer coefficients are plotted in Figures. (10 and 11) for two types of nanofluids (Ag + oil), and (TiO₂ + oil). There is a reasonable agreement between the two values. The overall heat transfer coefficient for counter flow was 6 – 12 % more than that of parallel flow at 5 wt % for two types of nanofluids(Ag + oil), and (TiO₂ +oil). The overall heat transfer coefficient for counter flow was 25 – 52 % more than that of parallel flow for two types of nanofluids (Ag + oil), and (TiO₂ +oil) with 30 wt % weight concentration. It is observed that there is no significant effect of heat transfer on changing flow condition. The reason is that the tube side primary flow and generation of secondary flow are always perpendicular to the shell side flow. Therefore, the change of flow direction does not affect overall heat transfer. The results from the counter flow configuration were similar to the parallel flow. Heat transfer rates, however, are much higher in the counter flow configuration, due the increased log mean temperature difference.

Figs. (12 – 15) exhibit the variation of inner Nusselt number versus Dean number for the flow of base oil and the nanofluids (Ag + oil and, TiO₂ + oil) with different nanoparticle weight concentrations. On comparing the parallel flow and counter flow configuration, it is found that there is no significant impact on inner Nusselt number when Ag, and TiO₂ – oil nanofluids are circulated. This is because

whatever be the flow configuration between shell and coiled tube, the inner heat transfer coefficient is the same. This means that the generation of centrifugal force and secondary flow did not get negative impact. It is also observed that the inner Nusselt number increases when particle concentration is higher. This is due to higher inner heat transfer coefficient and thermal conductivity. In general, higher the thermal conductivity, higher the convective heats transfer. The addition nanoparticle of silver and titanium oxide to the base oil has led to an increase in Nusselt number for flow inside helical tube. In general the addition of nanoparticles enhances the thermal conductivity of the base fluid. This enhancement in thermal conductivity would increase the convective heat transfer coefficient. As well as, chaotic movement of the nanoparticles in flow will disturb the thermal boundary layer formation on the tube wall surface. As a result of this disturbance, the development of the thermal boundary layer is delayed. Since, higher Nusselt number of nanofluid flow in a spiral tube are obtained at the thermal entrance region, the delay in thermal boundary layer formation resulted by adding nanoparticles will increase the Nusselt number. At higher weight concentrations of the nanofluids, both the thermal conductivity of the Ag, TiO₂ – base oil mixture and the disturbance effect of the nanoparticles will increase. Therefore, as it is expected, nanofluids with higher weight concentrations have generally higher Nusselt number.

Figs. (16 and 17) reveal the ratios of Nusselt number of nanofluids with 30 wt % to that of base oil as a function of Reynolds number for helical tube. It is observed that nanofluids (Ag + oil and, TiO₂ + oil) have better heat transfer performance when they flow inside helical tube. The results clearly show that at nearly the same range of Reynolds numbers, the highest Nusselt number ratios are obtained for the helical tube. For instance, a maximum increase of 34.15% (Ag + Oil) and 27.23% (TiO₂+ Oil) in Nusselt number ratio for a range of Reynolds numbers between 20 and 200 is obtained for the helical tube. This phenomenon could be due to the intensified chaotic motion of the nanoparticles inside helical tube. Since, the shear rate near the wall of the helical tube is high, the non – uniformity of the shear rate across the cross section will increase and therefore, the particles are more motivated by the variation of the shear rate. The measured pressure drop for the flow of base oil and Ag, TiO₂ + base oil nanofluids with different weight concentration as a function of Reynolds number along the helical tube is given in Figs. (18 – 21), respectively. The results exhibit that there is a noticeable increase in pressure drop of nanofluid with

5 wt % nanoparticle concentration compared to the oil value. This enhancement trend tends to continue for the nanofluids with higher weight concentration. This is because of the fact that suspending solid particles in a fluid generally increases dynamic viscosity relative to the base fluid. Since, the viscosity is in direct relation with pressure drop, the higher value of viscosity leads to increased amount of pressure drop. Another reason which can be responsible for pressure drop increasing of nanofluids may be attributed to the chaotic motion and migration of nanoparticles in the base fluid. This reason explains why at higher flow rates, the rate of increase in pressure drop has gone up while at very low Reynolds numbers, the pressure drops of base oil and nanofluids are almost the same. However, the rate of pressure drop increasing achieved for nanofluids with concentration ranges from 5 wt% to 30 wt % is less than that obtained when nanofluid with 5 wt% is used instead of oil. One reason for this behavior may be due to the anti – friction properties of Ag, TiO₂ nanoparticles. Ag, TiO₂ nanoparticles are basically spherical. The spherical shape of nanoparticles may result in rolling effect between the rubbing surfaces and the situation of friction is changed from sliding to rolling, thus the lubricant with nanoparticles achieves a good friction reduction performance. The rolling effect of nanoparticles was also reported by Battez et al. [28] and Wu et al. [29]. However, for the helical tube, the maximum pressure drop enhancement of 19.32 % (Ag + oil) and 13.42 % (TiO₂+oil) are achieved when nanofluid with 5 wt % concentration is used instead of base fluid.

When applying the heat exchanger with shell and helically coiled tube and using nanofluid flow inside the test sections instead of the oil flow, enhanced the convective heat transfer coefficient. However, these enhanced heat transfer techniques were both accompanied with increase in pressure drop which can limit the use of them in practical applications. Therefore, in order to find the optimum work conditions, a further study on the overall performance of these techniques should be carried out to consider pressure drop enhancement besides heat transfer augmentation, simultaneously. To do so, a new parameter called performance index, η , is defined as follows:

$$\eta = \frac{\left(\frac{Nu_{nf}}{Nu_{ht,bf}} \right)}{\left(\frac{\Delta p_{nf}}{\Delta p_{ht,bf}} \right)} \quad (10)$$

In which, Nu and ΔP represent Nusselt number and pressure drop of the flow resulted by applying enhanced heat transfer techniques, respectively. In addition, $Nu_{ht,bf}$ and $\Delta P_{ht,bf}$ are the Nusselt number and pressure drop of the base oil flow inside the helical tube, respectively. Apparently, when the performance index is greater than 1, it implies that the heat transfer technique is more in the favor of heat transfer enhancement rather than in the favor of pressure drop increasing. Therefore, the heat transfer methods with performance indexes greater than 1 would be feasible choices in practical applications.

Figs (22– 25) it is seen that the performance index is greater than 1 just for nanofluids with 5, 10, 20, and 30 wt % concentrations. The maximum performance index of 1.5 and 1.32 are obtained for the nanofluids (Ag + oil) and (TiO₂+oil) with 30 wt % concentration at Reynolds number of 190. Also It is seen from these figures that the, all concentration for the helical tube has performance indexes greater than 1. It means that for base flow along the helical tube, the rate of increasing in pressure drop is lower than increasing in heat transfer coefficient.

In addition, it is evident from Figs. (22, – 25) that applying helical tube is a more effective way to enhance the convective heat transfer compared to using nanofluids instead of the base fluid(oil). This relatively high performance index suggests that applying both of the heat transfer enhancement techniques studied in this investigation is a good choice in practical application.

Figs.(26 – 29) shows the flow curve shear stress is plotted against shear rate for Ag, and TiO₂ – oil nanofluids at ($\Phi= 5, 10, 20,$ and 30 wt %) particle weight concentration. The plot data for these types of nanofluid are not parallel, indicating that the materials are a Newtonian fluid over this range of shear stress. As well as these figure indicated the shear stress increases with an increasing shear rate, for Ag, and TiO₂ – oil nanofluids. These figures indicated the flow curve of the Ag, and TiO₂ – oil nanofluids measured using a spiral coil heat exchanger. The shear stress of nanofluids increases with an increase in concentration

of nanoparticles for both parallel flow and counter flow.

CONCLUSIONS

The conclusions can be drawn from the results of experimental study were as follows:

1. The shear stress of nanofluids increases with an increase in concentration of nanoparticles for both parallel flow and counter flow.
2. The type and size nanoparticles play an important role in enhancement of heat transfer rate.
3. No much impact of changing flow direction on overall heat transfer coefficient and the nanofluids (Ag, and TiO₂- oil) behaves as the Newtonian fluid for ($\Phi = 5, 10, 20,$ and 30 wt %).

4. The heat transfer characteristics in helical tube is better than oil by using Nanofluids .
5. Nanofluids that contain metal nanoparticles Ag, show more enhancements compared to oxide nanofluids TiO₂ – oil and compared with oil flow as well as the use of nanofluid (Ag, and TiO₂ – oil) significant gives higher Nusselt number than oil base fluid.
6. The performance index for the nanofluid flow inside the helical tube is greater than the performance index of the base oil flow. This relatively high performance index suggests that applying both of the heat transfer enhancement techniques studied in this investigation is a good choice in practical application.
7. The pressure drop of nanofluids in helical tube is greater than pressure drop of oil flow

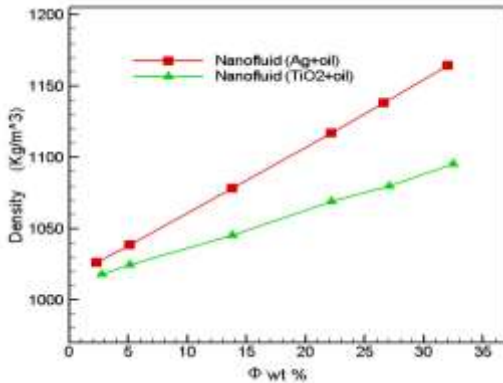


Fig 4. Density of nanofluids for (Ag+ oil) and (TiO₂+oil) at different weight fraction

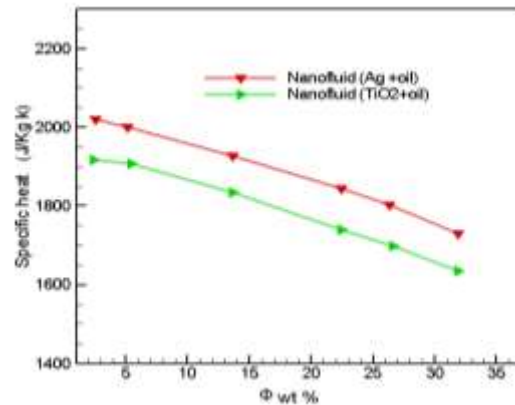


Fig 6. Specific heat of nanofluids for (Ag + oil) and (TiO₂+oil) at different weight fraction

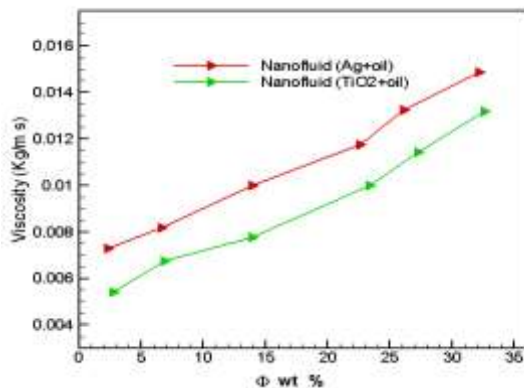


Fig 5. Viscosity of nanofluids for (Ag + oil) and (TiO₂+oil) at different weight fraction

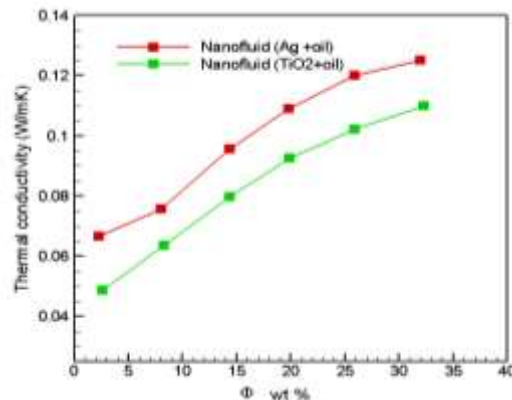


Fig 7. Thermal conductivity of nanofluids for (Ag + oil) and (TiO₂+oil) at different weight fraction

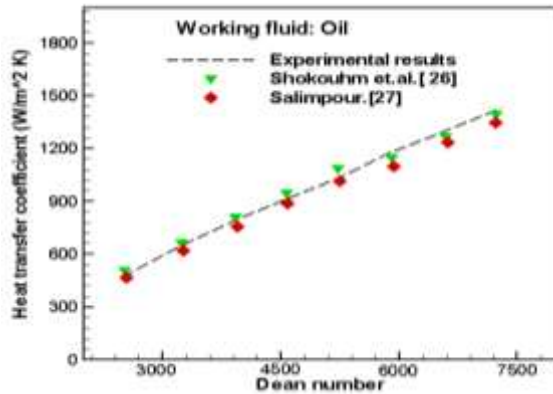


Fig 8. Comparison between measured heat transfer coefficient and that calculated from [26,27]

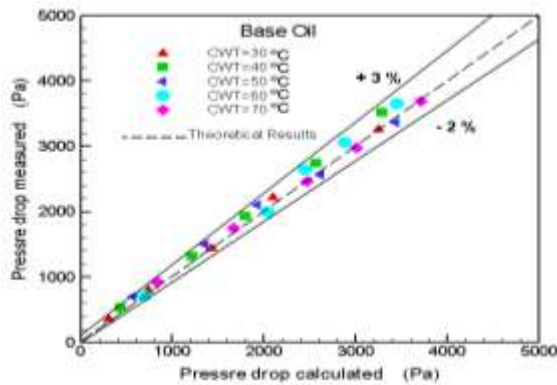


Fig 9. Comparison between theoretical and experimental pressure drop of base oil at CWT

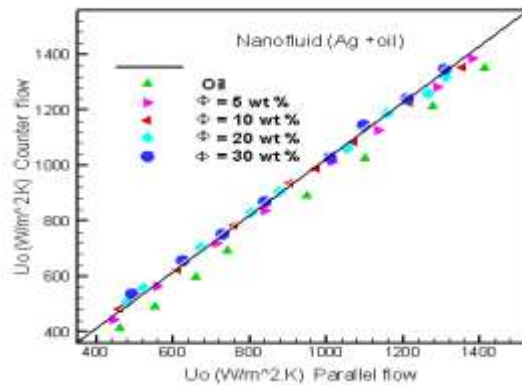


Fig 10. Comparison of overall heat transfer coefficient of counter and parallel flow configuration for Ag +oil nanofluid

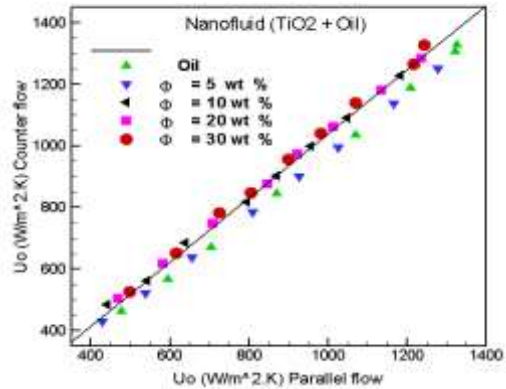


Fig 11. Comparison of overall heat transfer Coefficient of counter and parallel flow configuration for TiO₂+ oil nanofluid

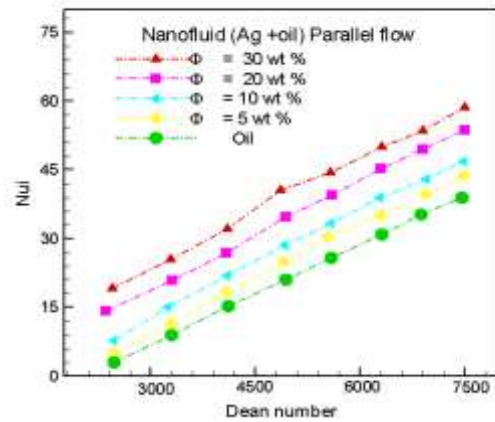


Fig 12. Variation of inner Nusselt number for nanofluid (Ag +oil) with parallel flow

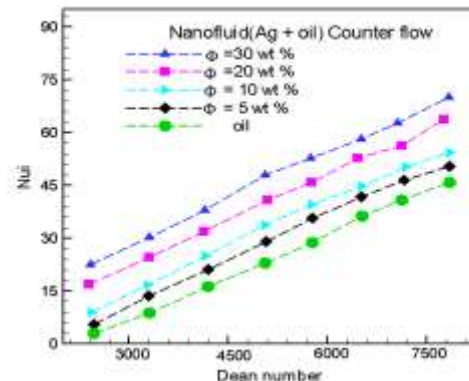


Fig 13. Variation of inner Nusselt number for nanofluid (Ag +oil) with counter flow

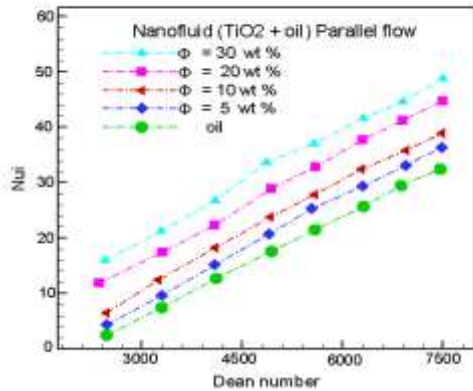
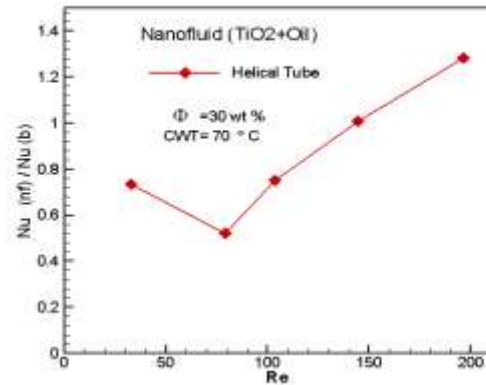


Fig 14. Variation of inner Nusselt number for nanofluid (TiO₂ +oil) with parallel flow



17. The Nu ratio versus Re to nanofluid (TiO₂ + oil) in helical tube at CWT and $\Phi=30$ wt %

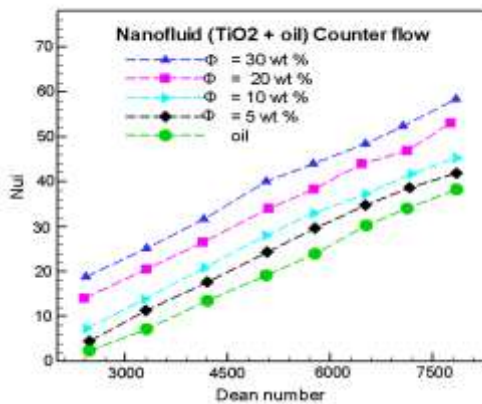


Fig 15. Variation of inner Nusselt number for nanofluid (TiO₂ +oil) with counter flow

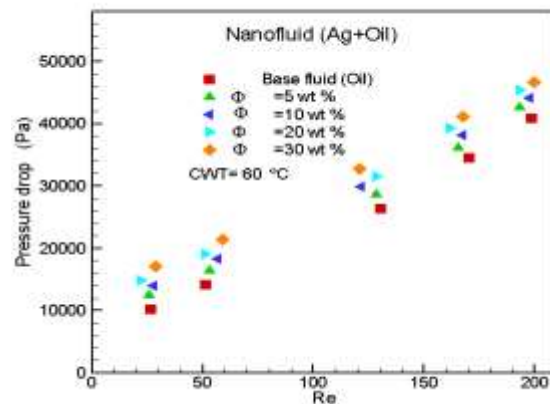


Fig 18. Pressure drop versus Re to nanofluid (Ag + oil) with parallel flow at different Φ and CWT

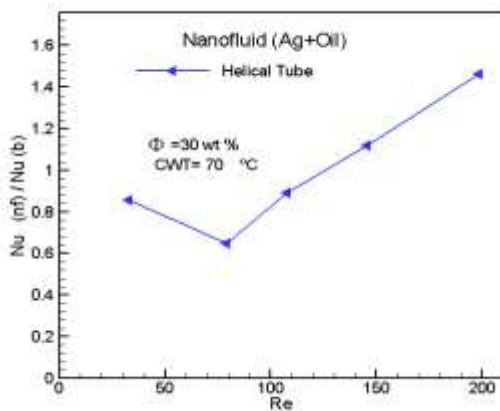


Fig 16. The Nu ratio versus Re to nanofluid(Ag + oil) in helical tube at CWT and $\Phi=30$ wt %

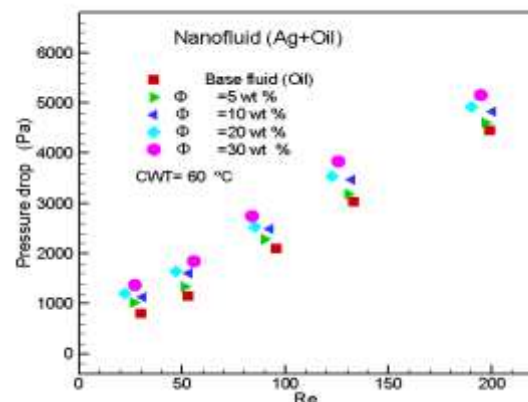


Fig 19. Pressure drop versus Re to nanofluid(Ag + oil) with counter flow at different Φ and CWT

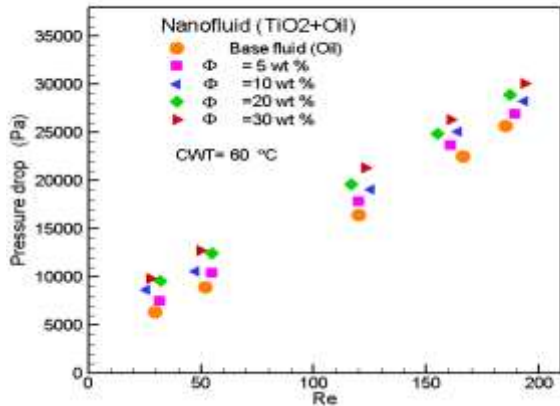


Fig 20. Pressure drop versus Re to nanofluid($TiO_2 + oil$) with parallel flow at different Φ and CWT

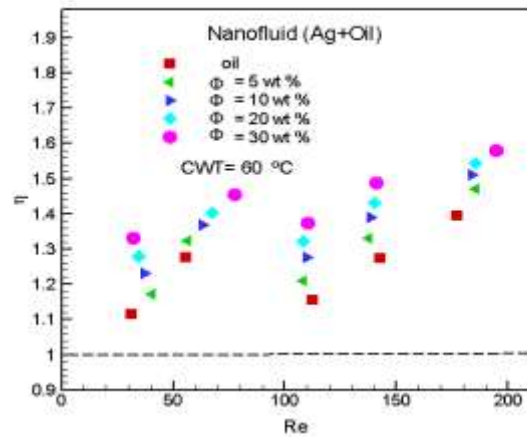


Fig 23. The performance index versus Re to nanofluid($Ag +oil$) with counter flow at different Φ and CWT

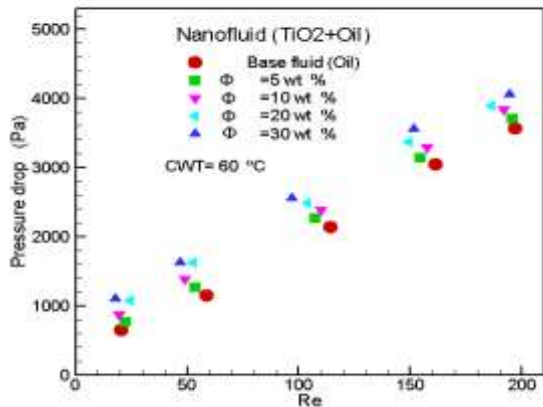


Fig 21. Pressure drop versus Re to nanofluid($TiO_2 + oil$) with counter flow at different Φ and CWT

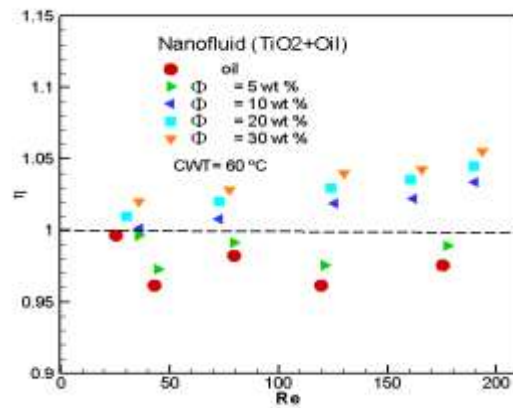


Fig 24. The performance index versus Re to nanofluid($TiO_2 + oil$) with parallel flow at different Φ and CWT

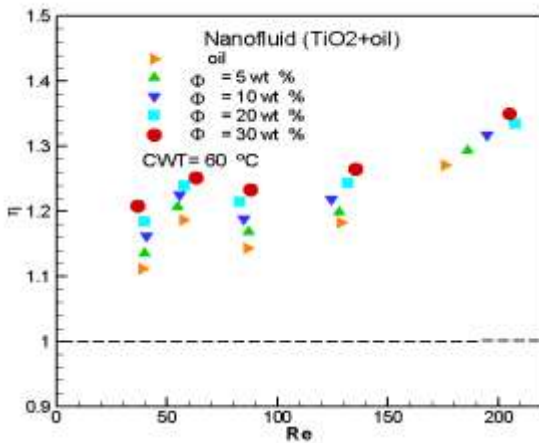


Fig 22. The performance index versus Re to nanofluid($Ag +oil$) with parallel flow at different Φ and CWT

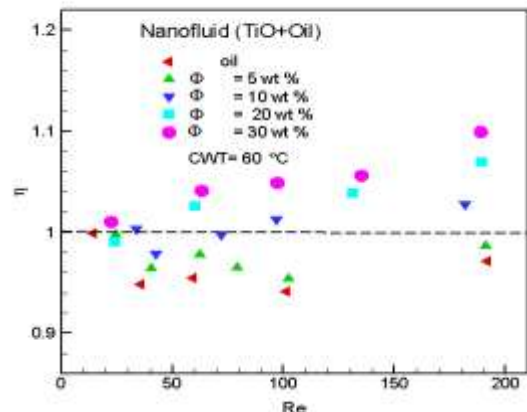


Fig 25. The performance index versus Re to nanofluid(TiO_2 + oil) with counter flow at different Φ and CWT

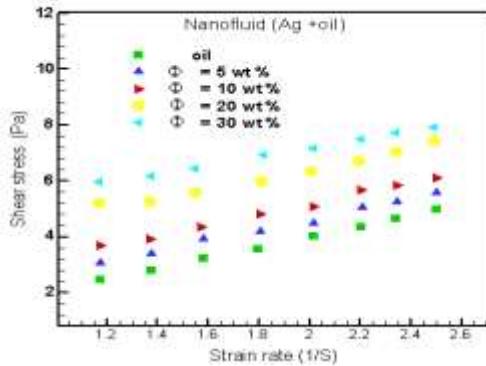


Fig.26. Shear stress versus shear rate for nanofluid (Ag +oil) with parallel flow

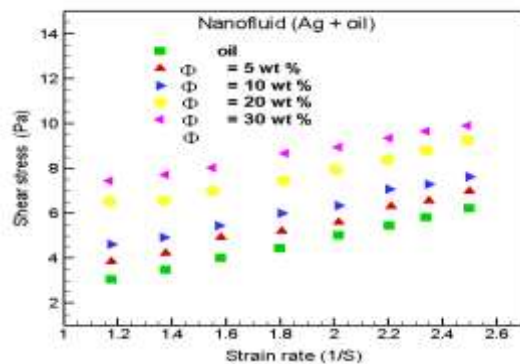


Fig.27. Shear stress versus shear rate for nanofluid (Ag +oil) with counter flow

REFERENCES

1. A.E. Bergles, Recent development in convective heat transfer augmentation, Applied Mechanics Reviews 26 , 675–682, 1973.
2. J.R. Thome, Engineering Data Book III, Wolverine Tube Inc, 2006.
3. S.U.S. Choi, Enhancing thermal conductivity of fluids with nanoparticles, ASME FED 231 , 99–105, 1995.
4. M. Chandrasekar, S. Suresh, A. Chandra Bose, Experimental investigations and theoretical determination of thermal conductivity and viscosity of Al_2O_3 /water nanofluid, Experimental Thermal and Fluid Science 34 , 210–216, 2010.
5. W. Yu, H. Xie, L. Chen, Y. Li, Enhancement of thermal conductivity of kerosene based Fe_3O_4 nanofluids prepared via phase-transfer method, Colloids and Surfaces A: Physicochemical and Engineering Aspects 355 , 109–113, 2010.
6. H.A. Mintsa, G. Roy, C.T. Nguyen, D. Doucet, New temperature dependent thermal conductivity data for water-based nanofluids, International Journal of Thermal Sciences 48 ,363–371, 2009.
7. R.S. Vajjha, D.K. Das, Experimental determination of thermal conductivity of three nanofluids and development of new correlations, International Journal of Heat and Mass Transfer 52 ,4675– 4682, 2009.
8. N.R. Karthikeyan, J. Philip, B. Raj, Effect of clustering on the thermal conductivity of nanofluids, Materials Chemistry and Physics 109, 50 –55, 2008.
9. S.M. Fotukian, M. Nasr Esfahany, Experimental study of turbulent convective heat transfer and pressure drop of dilute CuO /water nanofluid inside a circular tube,

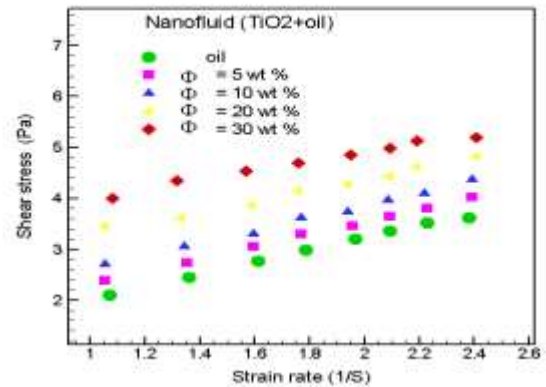


Fig.28 Shear stress versus shear rate for Nanofluid (TiO_2 + oil) with parallel flow

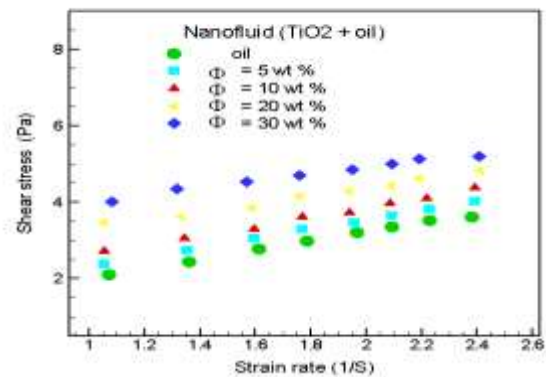


Fig. 29 Shear stress versus shear rate for nanofluid (TiO_2 + oil) with counter flow

- International Communications in Heat and Mass Transfer 37 ,214–219, 2010.
10. B. Pak, Y.I. Cho, Hydrodynamic and heat transfer study of dispersed fluids with submicron metallic oxide particle, *Experimental Heat Transfer* 11, 151–170, 1998.
 11. W.C. Williams, J. Buongiorno, L.W. Hu, Experimental investigation of turbulent convective heat transfer and pressure drop of alumina/water and zirconia/ water nanoparticle colloids (nanofluids) in horizontal tubes, *Journal of Heat Transfer* 130 2412–2419, 2008.
 12. Y. He, Y. Jin, H. Chen, Y. Ding, D. Cang, H. Lu, Heat transfer and flow behavior of aqueous suspensions of TiO₂ nanoparticles (nanofluids) flowing upward through a vertical pipe, *International Journal of Heat Mass Transfer* 50, 2272 – 2281, 2007.
 13. D. Wen, Y. Ding, Experimental investigation into convective heat transfer of nanofluids at the entrance region under laminar flow conditions, *International Journal of Heat and Mass Transfer* 47 ,5181–5188, 2004.
 14. Y. Ding, H. Alias, D. Wen, A.R. Williams, Heat transfer of aqueous suspensions of carbon nanotubes, *International Journal of Heat and Mass Transfer* 49, 240–250, 2006.
 15. Y. Xuan, Q. Li, Investigation on convective heat transfer and flow features of nanofluids, *Journal of Heat Transfer* 125 ,151–155, 2003.
 16. M. Chandrasekar, S. Suresh, A. Chandra Bose, Experimental studies on heat transfer and friction factor characteristics of Al₂O₃/water nanofluid in a circular pipe under laminar flow with wire coil Inserts, *Journal of Thermal and Fluid Science* 34 ,122–130, 2010.
 17. D.G. Prabhanjan, G.S.V. Raghavan, T.J. Rennie, Comparison of heat transfer rates between a straight tube heat exchanger and a helically coiled heat exchanger, *International Communication of Heat Mass Transfer* 29, 185–191, 2002.
 18. R.C. Xin, A. Awwad, Z.F. Dong, M.A. Ebadian, An experimental study of single phase and two-phase flow pressure drop in annular helicoidally pipes, *International Journal of Heat Fluid Flow* 18 ,482 – 488,1997.
 19. Choi, c., H.S. Yoo, and IM. Oh, Preparation and heat transfer properties of nanoparticle-in-transformer oil dispersions as advanced energy-efficient coolants. *Current Applied Physics*, 8(6): p. 710 – 712, 2008.
 20. US Research Nanomaterials, Inc. 3302 Twig Leaf Lane, Houston, TX 77084, USA Phone: (Sales) 832 – 460 – 3661 ; (Shipping) 832 – 359 – 7887 Fax: 281 – 492 – 8628 ,Service@us-nano.com ; Tech@us-nano.com
 21. Website, <http://WWW.CASTROL.COM/US> , Castrol (GTX) Company, BP Lubricants USA Oil Company, 46, USA,2014.
 22. Kumar, R., & Rosen, M. A.. Thermal performance of Integrated collector-storage solar water heater with corrugated absorber surface. *Applied Thermal Engineering*, 30, 1764-1768,2010.
 23. Das, S. K., Choi, S. U. S., Yu, W., & Pradeep, T. "Nanofluid Science and Technology". John Wiley & Sons, Inc., Publication, 2007.
 24. F.M. White, *Heat Transfer*, Addison-Wesley Publishing CompanyInc., New York, NY, 1984.
 25. Seban, R.A., Mclauchlin E.F., "Heat transfer in tube coils with laminar and turbulent flow", *Heat mass transfer* 6, 387-395, 1962.
 26. H.Shokouhm and, M.R. Salimpour, M.A. Akhavan – Behabadi , Experimental investigation of shell and coiled tube heat exchangers using Wilson plots,*International Communications in Heat and Mass Transfer* 35 ,84 – 92,2008 .
 27. M.R. Salimpour, Heat transfer characteristics of a temperature – dependent property fluid in shell and coiled tube heat exchangers, *International Communications in Heat and Mass Transfer* 35 ,1190 – 1195, 2008.
 28. A.H. Battez, R.G. alez, J.L. Viesca, J.E. Fernandez, J.M. Diaz Fernandez, A. Machado,R. Chou, J. Riba, CuO, ZrO₂ and ZnO nanoparticles as anti – wear additive in oil lubricants, *Wear* 265 (2008) 422–428.
 29. Y.Y. Wu, W.C. Tsui, T.C. Liu, Experimental analysis of tribological properties of lubricating oils with nanoparticle additives, *Wear* 262 (2007) 819–825.

NOMENCLATURE

Symbol	Quantity	units
CWT	Constant wall temperature	___
Cp	Specific heat	J/kg k
D	Tube diameter	m
d	Diameter of the coil	m
Nu	Nusselt number	--
Pr	Prandtl number	--
Re	Reynolds number	--
ΔP	Pressure drop	Pa
f	Friction factor	___
fc	Friction factor of coil	___
De	Dean number	___
U0	Overall heat transfer coefficient	W/m ² .K
kn	Thermal conductivity of nanofluid	W/m ² .K
Φ	Nanoparticle weight fraction	--
γ	Shear rate	s ⁻¹
	Greek Symbol	
μ_n	Dynamic viscosity Nano fluid	N.s/m ²
η	Performance Index	___
	Subscripts	
nf	Nanofluid	___
bf	Base fluid (oil)	___
ht	Helical tube	